ELSEVIER

Contents lists available at ScienceDirect

## Forest Ecology and Management

journal homepage: www.elsevier.com/locate/foreco





# Spatio-temporal vegetation and catchment dynamics following wildfires in the Southern Appalachian Ecoregion

I. Bouvier <sup>a,\*</sup>, P. Caldwell <sup>b</sup>, P. Houser <sup>a</sup>

- <sup>a</sup> George Mason University, 4400 University Drive, Fairfax, VA 22030, United States
- <sup>b</sup> USDA Forest Service, Southern Research Station, Center for Integrated Forest Science, Otto, NC 28763, United States

#### ARTICLE INFO

Keywords: Wildfires Southern Appalachian Ecoregion Catchment dynamics

#### ABSTRACT

This study used dense time-series satellite imagery, field data and historical streamflow records in a paired catchment approach to 1) estimate burn severity across a large ecoregion; 2) analyze vegetation recovery and 3) evaluate the effects of forest disturbance on annual water yield. While wildfire is an important driver of annual forest disturbance in Western United States, forest disturbance due to fire is infrequent in the Eastern United States. Changes in wildfire frequency and intensity amid climate variability are anticipated to increasingly impact forest ecosystems in regions with rare fire occurrence, and where fire effects on vegetation and watershed hydrology are under-studied. This research knowledge gap could impact managers that need dependable data and models to anticipate and plan for potential impacts on forested watersheds and water supply. Results from analysis of satellite time series within burned areas indicate post-fire vegetation decline and recovery in the largest wildfire perimeters. In a burned forested watershed, annual water yield was significantly impacted by forest disturbance, with an increase of up to 25 % in the years immediately following wildfire. These results are novel and significant for improving our understanding of infrequent wildfire impacts on vegetation recovery and water supply.

## 1. Introduction

Forests provide essential ecosystem services, including flowing water critical for the overall sustainability of a region and country (Valjarević, 2024), reducing the impact of high intensity rainfall and erosion, impact water quality downstream, and contributing to rainfall through evapotranspiration. As forests provide ecosystem services to expanding human populations, there is growing concern about decreased forest resilience amid disturbance compounded by climate change and variability. Emerging evidence suggests climate change contributes to significant disruption in forest ecosystems with the potential to alter forests beyond their potential ecological resilience, especially for temperate, tropical and arid forests (Seidl et al., 2017; Forzieri et al., 2022).

Drivers of forest disturbance can be related to natural (such as wildfire, drought, storms, tree pathogens,insect defoliators) or anthropogenic (such as harvesting, shifting agriculture) agents. The effects of forest disturbance can depend on possible interactions between disturbance agents and the ability of forest ecosystems to survive and even recover from disturbance over time (Forzieri et al., 2022). Among forest disturbances, wildfire depends on interactions with climate, vegetation,

terrain characteristics, and other factors, with the potential to cause lasting changes in forest ecosystems and resilience. The characteristics of vegetation are critical in determining fuel potential, with grassland and shrubland vegetation displaying lower fuel potential compared to forestland. Differences in tree age and species influence variability in fire burning potential (Vujović et al., 2024). Remote sensing, which includes satellite and aerial imagery, has a critical role in modern wildfire detection and characterization over large areas (Carta et al., 2023), with possible data gaps in regions with frequent cloud cover (Chen et al., 2024). Remotely sensed data has been used extensively to delineate fire perimeters and to characterize fire effects, especially to derive important metrics such as burned area and burn severity (Meng and Zhao, 2017).

Remotely sensed data has been used extensively to characterize fire effects, especially to derive important metrics such as burned area and burn severity (Meng and Zhao, 2017). Monitoring post-fire vegetation recovery is critical to understanding conditions that promote post-fire forest ecosystem resilience (Meng et al., 2015, Pérez-Cabello et al., 2021). However, widely used vegetation indices derived from remotely sensed data cannot easily distinguish between post-fire understory and

E-mail address: ibouvier@gmu.edu (I. Bouvier).

<sup>\*</sup> Corresponding author.

canopy vegetation recovery. Several studies found a relationship between fire burn severity and post-fire vegetation recovery (Zhao et al., 2016, Yang et al., 2017, Bright et al., 2019), with an initial variable increase in forest recovery by tree species and burn severity, underscoring the importance of combining remotely sensed and field data to understand the effects of fire severity on short and long-term tree mortality (Meng et al., 2018).

Experimental studies that specifically consider vegetation recovery in post-wildfire catchment hydrologic recovery remain rare, due to practical challenges associated with designing an experiment with concomitant large, prescribed fires attempting to reproduce wildfire behavior and vegetation impacts. In addition, few of the catchments that have been historically impacted by wildfires were instrumented at the time of the wildfires, and therefore there is a limited sample of catchments where retrospective analysis of wildfire impacts on streamflow is feasible using existing methods and tools. Several studies, including a synthesis of model-based approaches to predict water yield following wildfire (Partington et al., 2022) found that although impacts vary spatially and by ecoregion and hydrologic regime, incorporating burn severity and vegetation recovery can significantly improve streamflow prediction following wildfires. The findings strongly suggest the need for additional data and tools to support research and improvements in understanding the role of vegetation recovery and forest ecosystem resilience alongside post-wildfire catchment dynamics. This is particularly challenging in the case of infrequent wildfires, due to the lack of existing observations. Additionally, observed and predicted increased wildfire frequency could cause hydrological non-stationarity. This could impact the predictive power of existing models that rely on historical data records. This study's focus on understanding the impact of infrequent wildfires addresses this research gap and presents a rare opportunity to examine wildfire effects on vegetation and hydrologic recovery in the historically understudied Southern Appalachian Ecoregion.

Forest fires are infrequent in the Southern Appalachian/Blue Ridge Mountains Ecoregion (SAE) and therefore historically have not been considered a major driver of forest disturbance. The last period of SAE recorded widespread fires was associated with grazing and intense logging in the late 19th and early 20th century (Van Lear, 1989). However, historical evidence suggests that frequent -possibly annual fires shaped forest development, population growth, and land use change across the SAE long before the early 20th century logging operations and subsequent fire exclusion (Lafon et al., 2017). The relative dominance of fire-adapted tree species, such as oak (Quercus) and pine (Pinus) and especially the presence of endemic fire-resistance pine species such as the Table Mountain pine (P. pungens), is considered as evidence supporting a higher frequency of forest fires (Lafon et al., 2017). In late 20th century and early 21st century, SAE's forest composition has changed to favor mostly mesophytic (fire-intolerant) species, such as maples, in a shift from mostly xerophytic (fire-adapted) species (Elliott and Swank, 2008; Elliott and Vose, 2011). This shift in forest composition occurred in the context of fire exclusion and climate change, and sometimes following outbreaks of tree diseases and insect defoliators, such as the Chestnut blight and the Eastern hemlock. Following a summer-long severe drought period, the 2016 SAE wildfire outbreak was unprecedented in the amount of area burned and the number of reported suppressed ignitions (Caldwell et al., 2020; Reilly et al., 2022; Eidenshink et al., 2007). Occurring in the context of vegetation transition to mostly mesophytic species and increased variability, there is limited evidence regarding post-fire vegetation recovery and catchment dynamics in the SAE.

The purpose of this study was to enhance understanding of infrequent wildfire impacts on vegetation and catchment hydrological dynamics in the Southern Appalachian ecoregion. This study was focused on addressing the research knowledge gap through adapting methods in an under-studied region impacted by an infrequent wildfire event. This study had three objectives:1) to derive burn severity estimates based on dense remotely sensed image collections, informed by ground-based

measurements for the entire SAE; 2) to characterize post-fire vegetation recovery in wildfire-impacted areas; and 3) to evaluate possible post-fire hydrologic impacts in a watershed impacted by wildfire. The study represents a novel contribution to forest management through improved understanding of infrequent wildfire impacts on catchment dynamics. The study methods and findings enable managers to mitigate potential wildfire impacts in forested catchments, based on the ability to foresee and plan anticipatory catchment interventions.

#### 2. Methods

#### 2.1. Study area

The forests of Southern Appalachian/Blue Ridge Mountains Ecoregion (SAE) located in Southeastern U.S (Fig. 1) record some of the highest levels of biodiversity in North America (Anderson et al., 2013; Whittaker, 1956). The region covers a total area of 41,000 square kilometers, with a length of more than 1100 kilometers including diverse mountain ecosystems across the states of Virginia, North Carolina, South Carolina, Tennessee, and Georgia (Fig. 1). SAE's uniquely diverse forest ecosystems are characterized by a mix of coniferous trees, including a mix of pine (Pinus echinata) and deciduous oak forests at low elevations and a mix of mountain oak forests at moderate elevations (Arthur et al., 2021). At the highest elevations, spruce, fir, and northern hardwood are the most dominant tree species (Whittaker, 1956). The ecoregion experienced a decrease in total coniferous forest area in recent years, partly due to insect defoliators (Simon, 2005). The hemlock wooly adelgid infestation resulted in high tree mortality for Eastern hemlock (Tsuga canadensis) (Reilly et al., 2022). Since the mid to late 1970s, mountain forests in the Southern Appalachian region have undergone a shift from mostly xerophytic to mostly mesophytic tree species, which could decrease total water yield within a watershed (Caldwell et al., 2016).

## 2.2. Data and approach

This study used daily streamflow data for historical streamflow analysis and satellite image collections for pre and post wildfire vegetation condition analysis within watersheds impacted by the 2016 wildfires (Fig. 2, Methods).

#### 2.3. Wildfire burn severity

Across the Southern Appalachian Ecoregion, 21 wildfire perimeters with areas ranging between 219 and 11,194 hectareas, with a total area of 55,532 ha from the publicly available Monitoring Trends in Burn Severity (MTBS) 2016 perimeters were used to filter image time series using the cloud computing platform Google Earth Engine (Gorelick et al., 2017). The Harmonized Landsat Sentinel-2 (HLS) (Masek et al., 2021) surface reflectance and the Copernicus Harmonized Sentinel Level-1C orthorectified top-of atmosphere collection (European Space Agency, 2024; Gorelick et al., 2017) were accessed in Earth Engine over the entire Southern Appalachian Ecoregion for the growing season prior and following the 2016 wildfires (May-July 2016; May-July 2017). The Sentinel-2 Multi-Spectral Instrument (MSI) includes visible, near infrared and short-wave infrared bands. Frequent cloud cover in the Southern Appalachian Ecoregion may reduce the reliability of satellite data, thus Sentinel scenes at 30 m resolution were filtered by date and masked for < 20 % cloud presence in Google Earth Engine. The filtered image collection was reduced to a composite pixel value in each band representing the median value across all images in each pixel. The composite median reducer method mitigates quality issues related to residual cloud and shadow presence (Zhang et al., 2021). Advances in remote sensing enabled rapid wildfire detection from multiple platforms, including Landsat, Sentinel, NASA MODIS and Aqua. Future developments and multi-sensor data (SAR, LIDAR, optical, hyperspectral,

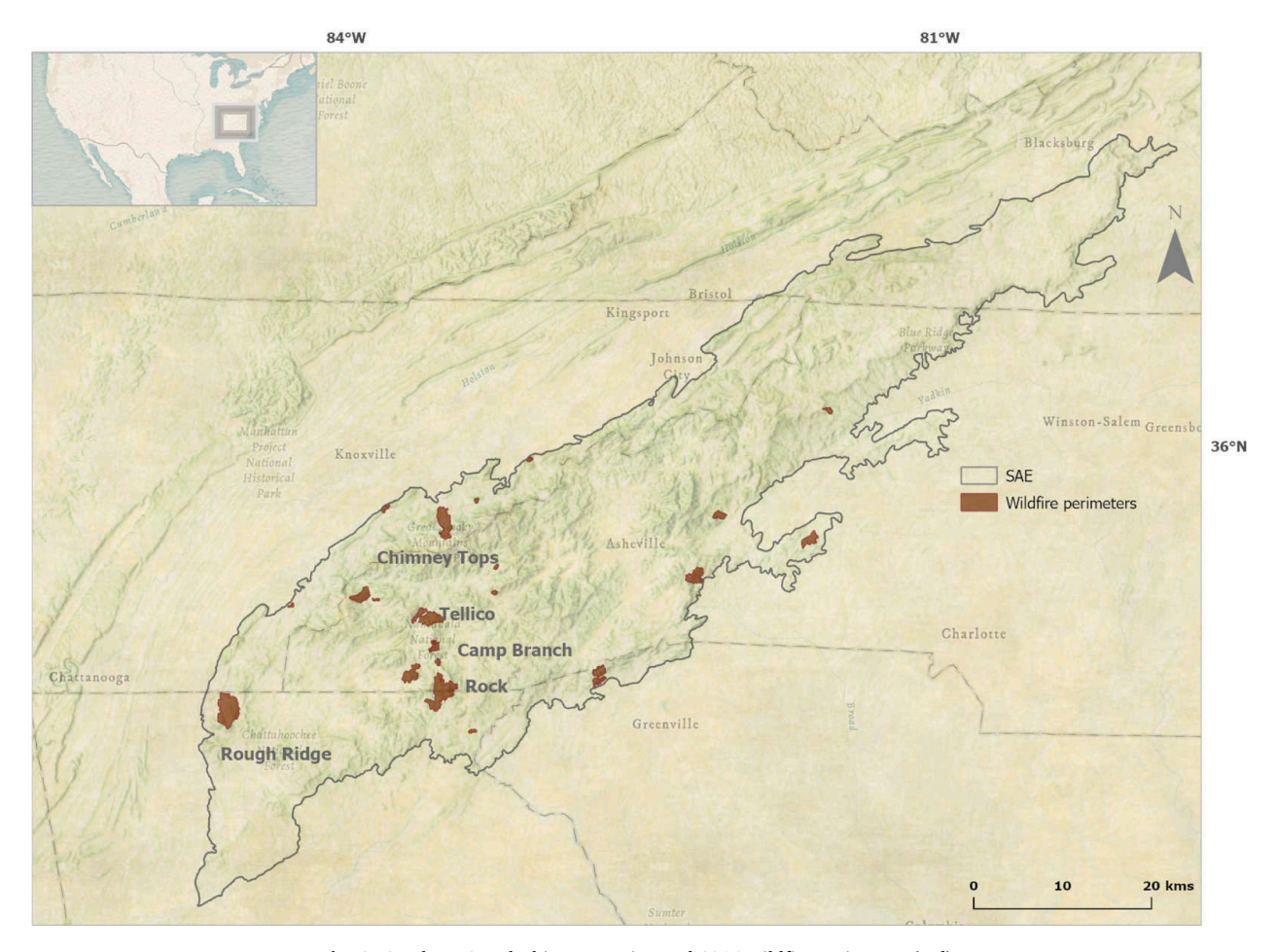


Fig. 1. Southern Appalachian Ecoregion and 2016 wildfire perimeters (red).

optical) fusion offer the potential to detect and characterize wildfires with greater accuracy (Yang et al., 2024).

The Normalized Burn Ratio (NBR) is the most common metric used to identify wildfire impacts and combines near infrared (NIR) and shortwave infrared (SWIR) reflectance (Eq. 1). Due to post-fire changes in NIR and SWIR reflectance, NBR is commonly used to identify fire signals in multispectral imagery and to estimate wildfire effects on vegetation. To identify the possible effects of wildfire on vegetation, post-fire NBR is subtracted from pre-fire NBR to calculate the differenced NBR (Key and Nathan, 2006) for a pair of images over the area of interest. A modified ratio, the relative dNBR (RNBR, Eq. 2) was introduced to improve fire signal detection (Miller and Thode, 2007). The workflow for RdNBR calculation is presented in Fig. 3.

$$NBR = \frac{(NIR - SWIR)}{(NIR + SWIR)}$$

NIR, SWIR are near and shortwave infrared bands

$$RdNBR = \frac{(NBRprefire - NBRpostfire)}{\sqrt{(|NBRprefire}|)}$$
 (2)

RdNBR calculated programmatically in Google Earth Engine was compared with plot-derived Composite Burn Index (CBI) based on variables measured following the 2016 wildfires at select field plots in Camp Branch and Tellico wildfires (Caldwell et al., 2020). The relationship between mean RdNBR derived from image collections and plot variables including tree mortality, basal area and char height was tested using Spearman's rank correlation coefficient. Watershed-level RdNBR was classified in burn severity categories using watershed-level RdNBR ranges (Caldwell et al., 2020). Low and moderate burn severity

categories were aggregated into one category, resulting in three burn severity categories: high, moderate, and low burn severity. Burn severity patches were further aggregated in contiguous patches with a minimum area of 5 ha. The level of agreement between plot-estimated burn severity and ecoregion mean RdNBR was evaluated with an accuracy matrix using a 10-meter buffer around plot locations.

Burn severity categories for the Southern Appalachian Ecoregion were combined with three elevation classes derived from the U.S Geological Survey 3D elevation program (USGS, 2020) at 1 m resolution: high elevation (>1000 m), medium elevation (500-1000 m), and low elevation (<500 m).

#### 2.4. Post-fire vegetation recovery

Post-fire vegetation recovery varies with pre-fire vegetation type, burn severity, topography and post-fire climate conditions (Meng et al., 2018, Zhao et al., 2016, Bright et al., 2019). Quantifying vegetation recovery can be challenging, due to a gap in metrics and methods that can be adapted to track vegetation recovery at high temporal resolution post-fire. However, recent advances in cloud computing and the growing availability of dense time series of medium and high-resolution multispectral imagery provide new opportunities for estimating recovery (Bright and all, 2019).

Two of the most popular indices used in estimating fire effects and vegetation change are the NBR and the Normalized Vegetation Index (NDVI, Eq. 3). NDVI is widely used in analysis of multispectral imagery.

$$NDVI = \frac{NIR - RED}{NIR + RED} \tag{3}$$

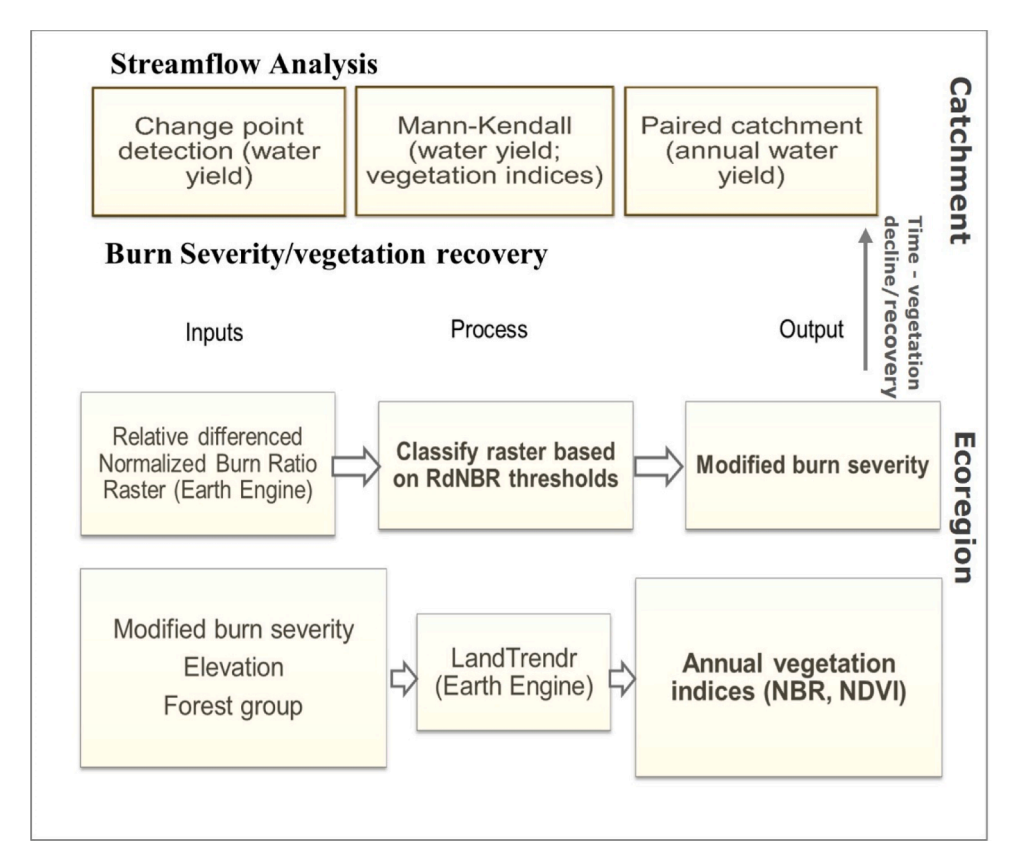


Fig. 2. Analytic methods overview.

A temporal segmentation algorithm, the Landsat-based detection of Trends in Disturbance and Recovery (Landtrendr) allows for fine-tuning of parameters to detect short and long-term changes in vegetation indexes over a Landsat time series and is well suited for detection of vegetation changes at fine time scales (Kennedy et al., 2010). The computationally intensive Landtrendr algorithm involves the creation of spectral trajectories across dense image series. A recent revision and implementation of Landtrendr in the cloud computing platform Google Earth Engine significantly reduces processing time and costs to identify breakpoints and spectral trajectories associated with forest disturbance over time (Kennedy et al., 2018).

The Landtrendr algorithm in Google Earth Engine was used to develop annual NBR and NDVI mean values and fitted values for all 2016 wildfire perimeters. Fire patches corresponding to high and moderate burn severity from four wildfire perimeters with the highest burn severity were stratified by elevation classes (<500 m, 500–1000 m, >1000 m). Landtrendr fitted trajectories were calculated based on a spatial sample in stratified patches. NBR annual percentage from average pre-fire NBR values was used to estimate vegetation recovery. The NBR percentage for each year was calculated as the fitted annual value divided by the pre-fire mean NBR levels.

NBR and NDVI time series over select patches in four wildfire perimeters with the highest burn severity were tested for significance of trends using Mann-Kendall or Kendall's tau test (Mann, 1945; Kendall, 1948). Mann-Kendall is used to test the null hypothesis that the data is independent and identically distributed in a time series. If the test results are significant, the null hypothesis is rejected and an increasing or decreasing monotonic trend is determined.

#### 2.5. Historical streamflow analysis

Although the paired watershed approach historically led to critical hydrologic findings (Burt and McDonnell, 2015), this method requires a

similarly long historical record of daily, quality-approved USGS reference watershed (Lins, 2012) streamflow records across selected watersheds.

The watersheds most impacted by 2016 wildfires across the region are the headwaters of the Nantahala River and watersheds drained by Tallulah River, West Pigeon River, Lower Cartoogechaye, Tellico, Shooting Creek, and Betty Creek. However, fire perimeters rarely overlap with gauged watersheds, making analysis of fire effects on the streamflow regime extremely challenging. Across our study area, we found one gauged watershed with a continuous record of daily streamflow pre-fire and post-fire that had more than 20 % of area within a burned perimeter. The 152.3 km² Tallulah watershed above the USGS station 02178400 near Clayton, GA was selected for historical streamflow analysis based on 35 % of its area within the Rock Mountain fire perimeter and the availability of historical data records. USGS historical daily streamflow data was accessed in R using the USGS data retrieval package (De Cicco et al., 2024) and the fasstr package (Goetz, Schwarz., 2023).

## 2.6. Paired watershed analysis

Two empirical methods were used to examine possible hydrologic impacts following the 2016 wildfire in Tallulah River catchment. For both methods, the unburned watersheds Chattooga above the USGS station 02177000 and Hiwassee above the USGS station 03544970 were selected as reference watersheds in a paired watershed approach (Table 1, Fig. 4). The Rock Mountain fire perimeter overlaps with 35 % of Tallulah watershed's area (Fig. 4).

All three watersheds are considered reference watersheds and thus have minimal anthropogenic flow alteration (Falcone, 2011).

Daily streamflow records from the pre-fire (2006–2016, Chattooga; 2008–2016, Hiawassee) and post-fire (2016–2023) were used for the paired watershed analysis.

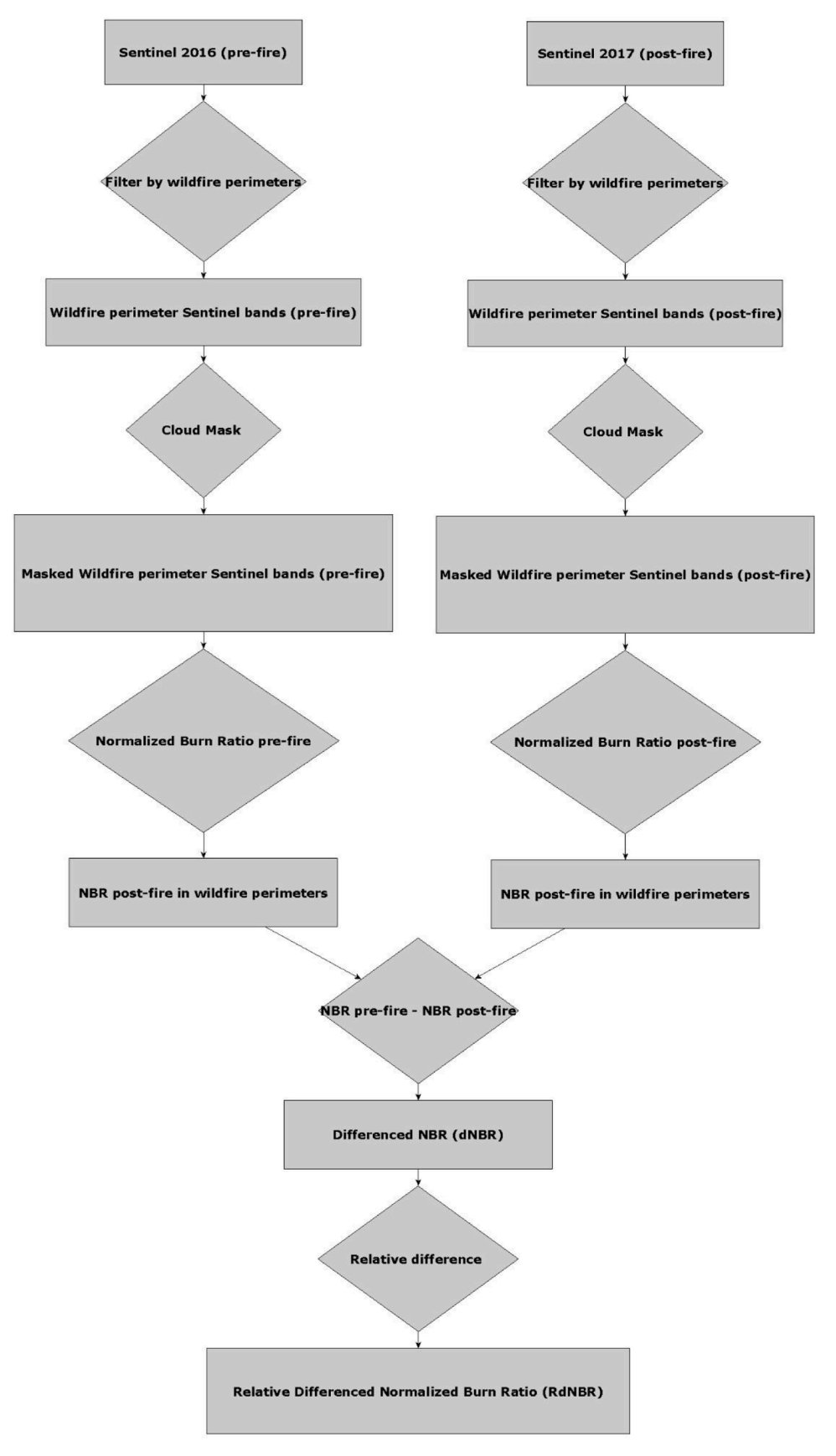


Fig. 3. RdNBR workflow.

**Table 1** Watershed characteristics.

Characteristics	Tallulah (burned)	Watershed Chattooga (unburned)	Hiwassee (unburned)
Total area (ha)	15,125	53,613	10,230
Mean elevation (m)	885	759	868
Mean slope (%)	22	18	21
Aspect	S	S	NW
Oak/Hickory Forest Group (%)	95	75	99
Mean water yield (Q, mm/year)	1002	947	1000

The first method, double-mass paired watershed analysis (Searcy andClayton, 1960; Biederman et al., 2015) is a visual method that compares the slope of cumulative flow in the burned watershed against the expected flow based on the relationship between streamflow in the two-watershed pre-fire. The difference between observed cumulative streamflow and the expected streamflow as annual residuals represents the streamflow effect of wildfire.

The second method involves developing a linear regression between the treatment (i.e., burned) and reference (i.e., unburned) watershed annual water yield (mm/year) prior to the treatment (fire), and using that relationship to estimate the expected annual water yield post-treatment in the treatment watershed had the treatment (fire) not occurred. Prediction intervals are then computed for each year at  $\alpha = 0.05.$  Numerous examples can be found in the literature that use this method to evaluate the effect of forest disturbance, such as harvest treatment or other disturbance on annual water yield (Ford et al., 2011, Swank et al., 2014, Srivastava et al., 2020).

## 2.7. Analysis of streamflow trends

Historical streamflow records at USGS Tallulah station near Clayton were analyzed to develop a complete flow history and metrics to examine trends in daily recorded streamflow. Trends in over 50 streamflow metrics were tested for significance using the Mann-Kendall non-parametric test of significance for the period prior and following the 2016 wildfires. A Bayesian ensemble model for detection of change

points in time series data (RBeast, Zhao et al., 2019) was used to analyze annual streamflow at Tallulah, Hiwassee, and Chattooga stations.

#### 3. Results

#### 3.1. Burn severity

The RdNBR model derived programmatically from time series of Sentinel imagery in Google Earth Engine was used to evaluate burn severity across the entire ecoregion.

Mean RdNBR was positively correlated with plot-measured tree mortality ( $r_s$ =0.76) and basal area loss ( $r_s$ =0.73). Threshold values for watershed-level RdNBR range (Caldwell et al., 2020) were used to classify burn severity, and the resulting moderate and low moderate classes were aggregated into a low burn severity class.

Modified threshold values were derived based on the distribution of RdNBR values at 60 plot locations, with values in the 25th percentile corresponding to the low severity class and values in the 75th percentile corresponding to the high severity class (Table 2).

Field-determined categorical burn severity at sampled plot locations in Tellico and Camp Branch fire perimeters was compared with burn severity derived from Sentinel-based RdNBR values. Categorical burn severity was compared using a 10-meter buffer around the plot locations. For watershed-level thresholds (Caldwell et al., 2020), agreement with aggregated plot burn severity categories was 80 % for low severity, 30 % for moderate severity, and 77 % for high burn severity categories.

**Table 2**Burn severity RdNBR thresholds.

Burn Severity Categories	High	RdNBR range (% agreement with plot categorical severity based on confusion matrix) Moderate	Low
Thresholds based on Caldwell et al. (2020)	> 542 (77 %)	62–541 (30 %)	< 62 (80 %)
Modified thresholds	> 492 (71 %)	201–491 (66 %)	< 200 (36 %)

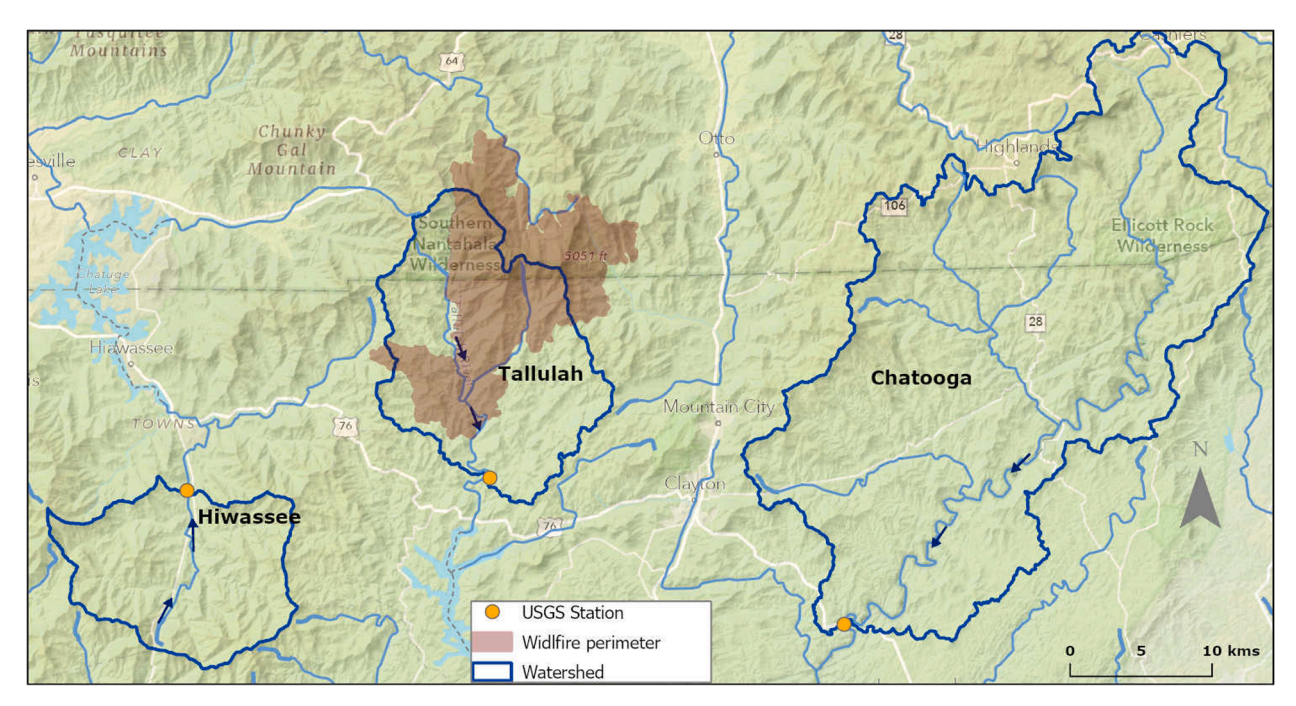


Fig. 4. Map of Tallulah, Hiwassee, and Chattooga watersheds.

**Table 3**Mann-Kendall test results for NBR and NDVI fitted values (2000–2016) in 2016 burned perimeters –Chimney Tops, Tellico, Camp Branch, and Rock Mountain.

Wildfire	NDVI fitted tau	NDVI <b>pvalue</b>	NBR fitted tau	NBR fitted pvalue
Chimney Tops	-0.05	0.822	-0.667	0
Tellico	0.7	0	0.067	0.753
Camp Branch	1	< 0.0001	-0.517	0.006
Rock Mountain	0.667	0	-0.783	< 0.0001

For modified threshold values, agreement with aggregated plot burn severity categories was 36 % for low severity, 66 % for moderate severity, and 71 % for high burn severity. Over 55 % of high burn severity areas were located at higher elevations, and 40 % at medium elevation.

A summary of the confusion matrix level of agreement for watershed-level thresholds and the modified RdNBR thresholds is presented in Table 2.

Burn severity was subsequently scaled up to the entire ecoregion using modified RdNBR thresholds for the three burn severity categories. Rock Mountain (18 %), Tellico (9 %), Camp Branch (29 %), and Chimney Tops (35 %) wildfire perimeters (Fig. 5) had the largest proportion of high burn severity areas within SAE fire perimeters overall. These perimeters are in a central SAE section (Fig. 5). Across all SAE fire perimeters, 13 % of the area was burned at high severity, 30 % at moderate severity, and 55 % at low severity.

#### 3.2. Post-fire vegetation recovery

Over a 23 years period, annual NBR shifted from significantly increasing during the pre-fire period to significantly decreasing post-fire in the Chimney Tops, Camp Branch, and Rock Mountain wildfire perimeters (Table 3 and 4). Although indicative of vegetation recovery, significant increasing post-fire monotonic NBR trends do not differentiate between forest and other vegetation recovery, such as grass or shrubs.

Time-series analysis of vegetation indices indicate a decline in growing season vegetation growth one-two years post fire, followed by vegetation recovery to 95 % of the pre-fire levels at the two- and three-years mark. The NBR trajectories show a clear decline following the 2016 wildfires for all major wildfire perimeters, with the largest magnitude in NBR decrease at Chimney Tops (Fig. 6). NDVI response is more muted, with only Chimney Tops showing a change in NDVI trajectory following the wildfires (Fig. 7). This is consistent with numerous studies indicating that NDVI is less sensitive to post-fire vegetation changes when compared to NBR (Bright et al., 2019, Pickell et al., 2016, Hislop et al., 2018).

Vegetation recovery is more nuanced when wildfire perimeters are classified by elevation classes and burn severity. Trajectories of estimated percentage of NBR recovery in stratified samples within four wildfire perimeters suggest relatively rapid recovery across all categories and elevation classes (Fig. 8). Camp Branch, Chimney Tops, and Rock Mountain had the highest decline in post-fire vegetation growth. Recovery in areas of high burn severity at elevation classes > 1000 m and 500–1000 m was slower than for areas of moderate burn severity, with an estimated 20 % of the area pre-fire still unrecovered seven years following the wildfires.

Since the highest variability in dominant forest type/group was in the Rock Mountain wildfire perimeter, a second set of fire perimeter patches for Rock Mountain were stratified by burn severity, dominant forest type, and elevation class. In Tallulah watershed, a drop in pre-fire NBR is evident in 2017 immediately following wildfires, with the highest decrease in areas of high burn severity located at 500–1000 m. NBR recovery post 2017 was detectable in all burned areas in Tallulah/

Rock Mountain wildfire perimeter, with differences in the rate of recovery between classes of different burn severity, elevation, and vegetation/forest group (Fig. 9). The pine forest group within high burn severity areas had the most consistent upward trend following the first year after wildfire. Post-fire NBR recovery within the dominant Oak/Hickory Forest group (Table 1) was similar for medium burn severity areas regardless of elevation, while stagnating until 2019 in areas of high burn severity. All burned areas showed similar recovery trends at five years following the wildfires. Five years post-fire, the NBR difference from pre-fire NBR indicator of vegetation growth was less than 5 % in all burned areas (Fig. 9).

NBR indicative of vegetation growth returned to 95 % of pre-fire levels in all burned areas within five years and returned fully to pre-fire levels by year seven (Fig. 10).

#### 3.3. Tallulah River historical streamflow analysis

The gauged Tallulah watershed provided an opportunity to examine potential impacts of the Rock Mountain fire on water yield and subsequent recovery. Approximately 35 % of the gauged watershed was within the Rock Mountain fire perimeter, and approximately 13 % of the watershed area was burned at high severity (Figs. 4 and 9). Paired catchment analysis comparing the burned Tallulah and unburned Chattooga and Hiwassee watersheds revealed a departure from expected cumulative annual streamflow following the 2016 wildfire event (Fig. 11, double mass analysis). The null hypothesis tested states that the slopes are equal between regression lines for the expected and the observed streamflow in the years following the wildfire event. Based on analysis of covariance (Biederman et al., 2015), the null hypothesis was rejected, and the slopes are significantly different.

The fit between the annual water yield of the burned Tallulah watershed and the unburned Chattooga watershed in the pre-fire period (2006–2016) was determined using linear regression (equation 4,  $R^2$ =0.92). Using this relationship and the annual water yield of the unburned Chattooga watershed, we estimated the expected annual water yield of the burned Tallulah watershed had the fire not occurred. The difference between the observed and expected water yield of the burned Tallulah watershed post-fire was then calculated (Fig. 12). These results show that a significant increase in annual water yield was observed in the burned Tallulah watershed in 2019, 2020, and 2021, after which the difference between observed and expected was not significant. The increase in annual water yield after the fire peaked in 2020 at + 378 mm, or 25 % greater than expected. Recovery of annual water yield occurred by 2022, approximately six years after the fire and three years after the initial significant increase in water yield.

QTallulah = 0.7\*QChattooga + 287.2 (equation 4) QTallulah is annual water yield for the burned watershed Tallulah and QChattooga is the annual water yield for the unburned Chattooga watershed

Similarly, the fit between the annual water yield of the burned Tallulah watershed and the unburned Hiwassee watershed in the pre-fire period (2006-2016) was determined using linear regression (equation 5,  $R^2$ =0.97). Using this relationship and the annual water yield of the unburned Hiwassee watershed, we found a significant increase in annual water yield in the burned Tallulah watershed in 2018, 2019, and 2020 when compared with Hiwassee watershed. After 2020, the difference between observed and expected was not significant (Fig. 13). The annual increase in water yield after the fire peaked in 2020 at + 295 mm, or 22 % greater than expected. Recovery of annual water yield occurred by 2021, approximately five years after the fire and three years after the initial significant increase in water yield. The annual increase in water yield after the fire peaked in 2020 at + 295 mm, or 22 % greater than expected. Recovery of annual water yield occurred by 2021, approximately five years after the fire and three years after the initial significant increase in water yield (Fig. 13).

 $\label{eq:QTallulah} QTallulah = 0.7*Q\emph{Hiwassee} + 287.2 \ (equation \ 5) \ Q\emph{Hiwassee} \ is \ the \\ annual \ water \ yield \ for \ the \ unburned \ watershed \ Hiwassee$ 

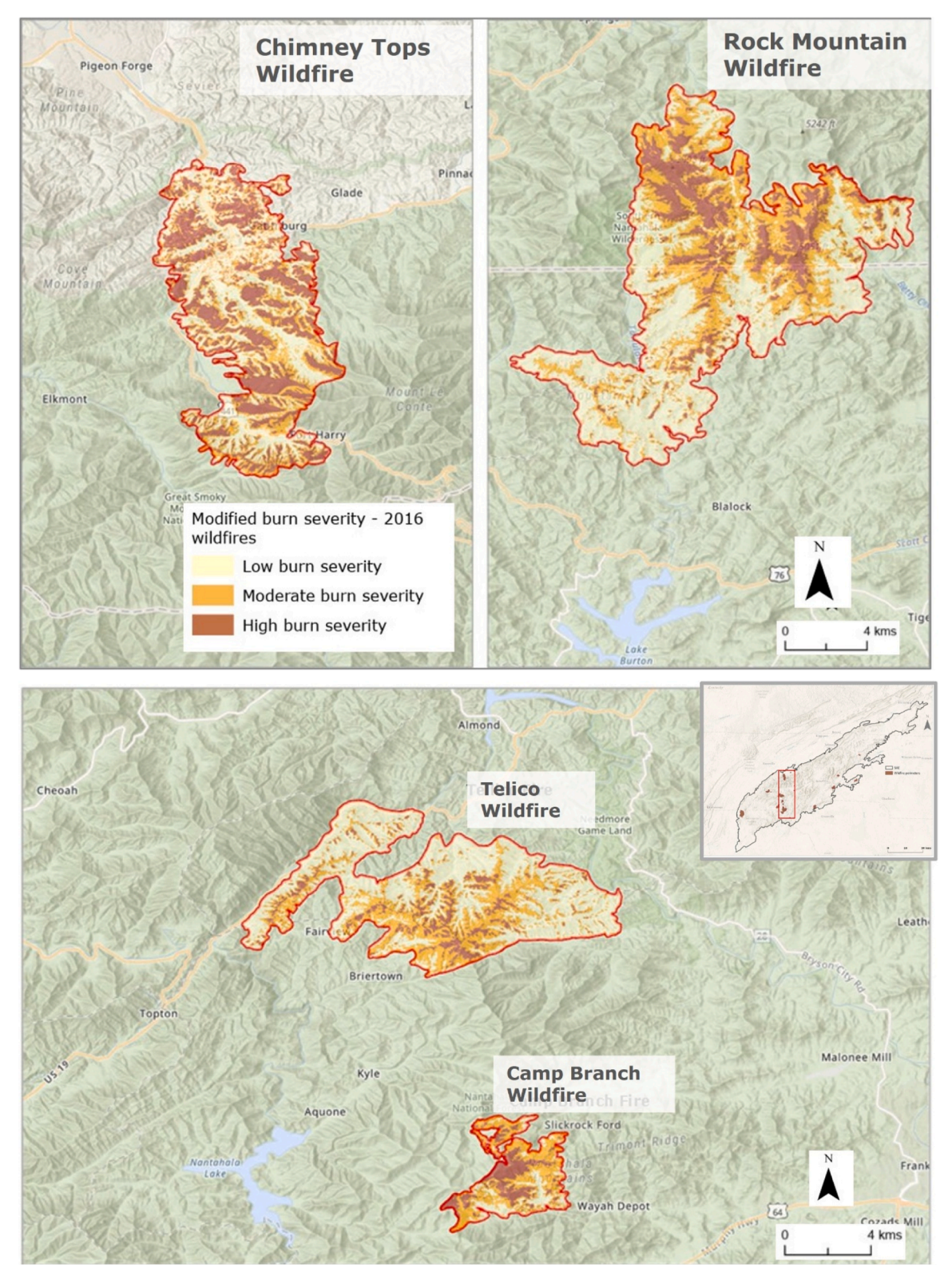


Fig. 5. Burn severity categories based on modified RdNBR thresholds - Chimney Tops, Rock Mountain, Tellico and Camp Branch fire perimeters.

Results from a change point detection analysis for Tallulah and paired watersheds Chattooga and Hiwassee indicate a significant positive trend change point detection at Tallulah in 2018. No significant change points were found at Chattooga for the period 2006–2023 or for Hiwassee for the period 2008–2023.

## 4. Discussion

The 2016 wildfire event in the Southern Appalachian Ecoregion was unprecedented in recent wildfire records for the Eastern United States, resulting in an estimated total burned area of over 60,000 ha (Reilly et al., 2022). This study found that half of SAE wildfire perimeters had

**Table 4**Mann-Kendall test results for NBR and NDVI fitted values (2016–2023) in 2016 burned perimeters –Chimney Tops, Tellico, Camp Branch, and Rock Mountain.

Wildfire	NDVI fitted tau	NDVI <b>pvalue</b>	NBR fitted tau	NBR fitted pvalue
Chimney Tops	1	0.009	1	0.009
Tellico	0.867	0.024	0.867	0.024
Camp Branch	0.867	0.024	1	0.009
Rock Mountain	1	0.009	1	0.009

only low or moderate burn severity areas, suggesting possible effective fire suppression methods and conditions potentially unsuitable for widespread, high severity fires. Within the larger wildfire perimeters, over half of high burn severity areas were located at higher elevations (above 500 m). The empirical relationship between plot-derived composite burn index (CBI) and burn severity derived from satellite imagery can present methodological challenges, especially over large areas with multiple fires. CBI assembles multiple variables, while RdNBR is derived from image time-series (Cardil et al., 2019). While burn severity classification models have been tested and scaled at watershed scale in the Western US, this approach presents limitations in the case of Eastern US wildfires, due to the paucity of field observations in regions with smaller wildfire perimeters. This study leveraged field observations and watershed-level RdNBR classification thresholds (Caldwell et al., 2020) to classify a composite NBR index derived from a collection of images. Modified thresholds resulted in higher levels of agreement with high burn severity categories. While the field data distribution is constrained to a small part of SAE, this overlaps with the central area most impacted by the 2016 wildfires. Further field data collection in watersheds impacted by infrequent wildfires will be needed to improve burn severity classification and transferability to other regions.

Results from comparison of high burn severity categories based on RdNBR programmatic calculations using cloud computing and image collection stacks show high agreement with plot-estimated burn severity. Changes in the threshold values resulted in higher overall agreement with plot CBI, with the lowest agreement, 30 % for areas of low severity, primarily due to confusion between the moderate and low

burn severity classes. This study's novel approach linked infrequent forest wildfire disturbance to changes in catchment dynamics in SAE, a region where forest wildfires have been understudied.

#### 4.1. Vegetation recovery after wildfires

This study found that five of the fire outbreaks resulted in significant decline in spectral reflectance after the fire, indicating growing season vegetation decline. A temporal decline in vegetation spectral reflectance was significant within fire perimeters burned at high and moderate burn severity, followed by rapid vegetation spectral reflectance increase, largely consistent with existing literature for wildfires and vegetation recovery (Wimberly, Reilly.,2007). However, initial vegetation spectral decline from pre-fire levels was only around 10 % from pre-fire levels even for fire perimeters with higher burn severity, which is less than other wildfire studies (Bright et al., 2019, Meng et al., 2018). In Tallulah watershed, estimated time to 95 % and 100 % recovery to annual pre-fire spectral NBR was 3–5 and 4–7 years, respectively.

The recovery was found to be shorter than in most other studies focused on Western U.S wildfires (Guz et al., 2022, Meng et al., 2018, Zhao et al., 2016). A reasonable explanation for this difference in recovery time is related to the fact that biomass accumulation and post-disturbance forest recovery is influenced by climatic factors (Anderson et al., 2006) with slower recovery in arid forests and in colder, more humid forests as compared to Southern Appalachian forests.

Post-fire vegetation recovery can be challenging to quantify due to limitations in distinguishing between shrub and grass recovery from forest recovery, especially following intense forest wildfires. It was beyond the scope of this study to collect ground truthing data across the southern Appalachian wildfires to validate the remotely sensed recovery and to separate recovery according to vegetation type. The absence of ground data collection is a limitation of this study but could be alleviated using remotely sensed data and leveraging known differences between forest and grass or shrub recovery. Given sufficient time, forest impacted by wildfire will eventually recover in several stages. Therefore, time since wildfire can be used to determine vegetation recovery and is a key factor in predicting post-fire vegetation recovery (Bartels

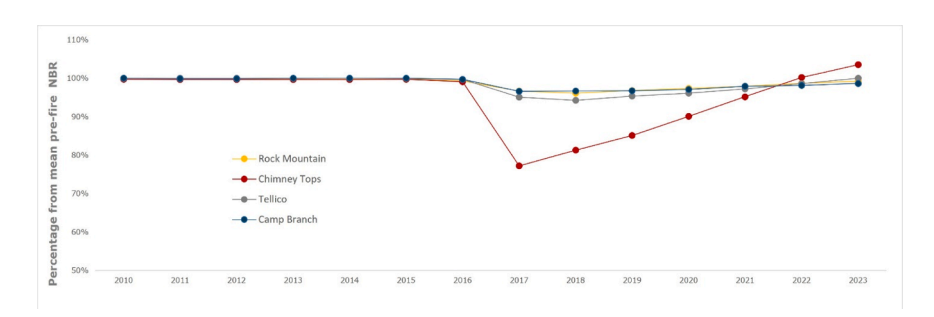


Fig. 6. NBR median and vegetation recovery in 2016 burned perimeters – Camp Branch, Chimney Tops, Rock Mountain, Tellico.

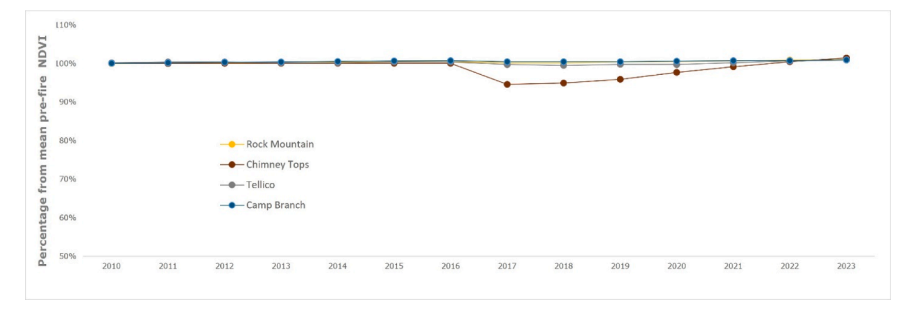
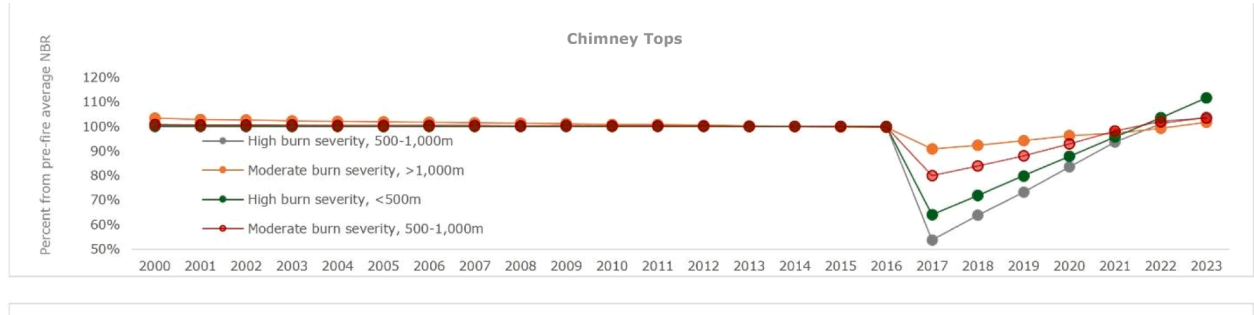
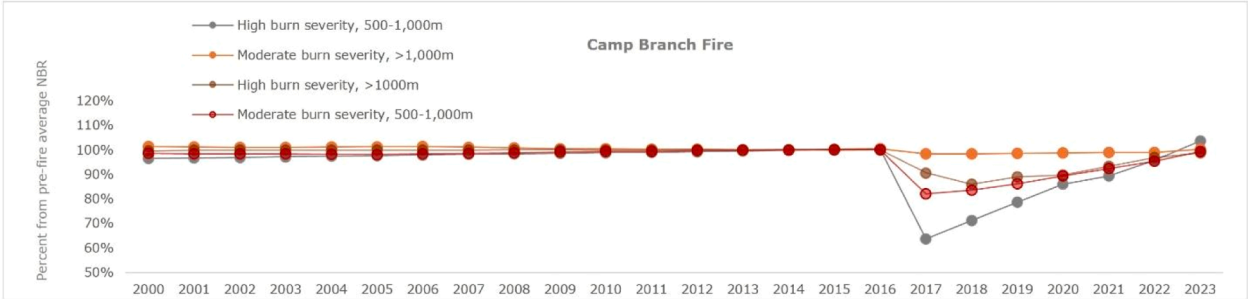
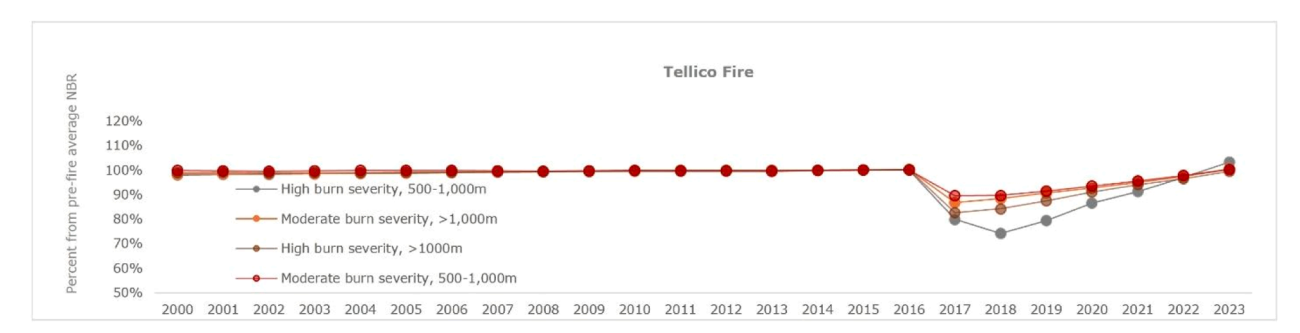


Fig. 7. NDVI median and vegetation recovery in 2016 burned perimeters -Camp Branch, Chimney Tops, Rock Mountain, Tellico.







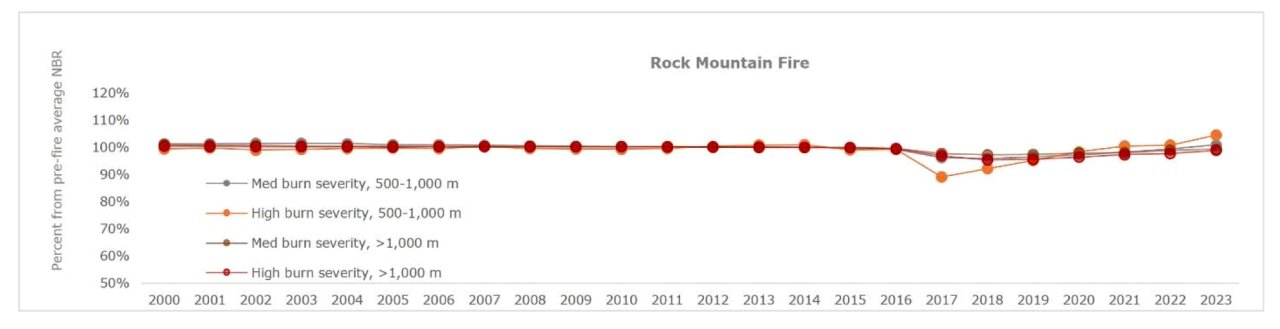


Fig. 8. Percent of annual fitted NBR values from pre-fire mean values in sampled pixels stratified by burn severity and elevation within four SAE wildfire perimeters.

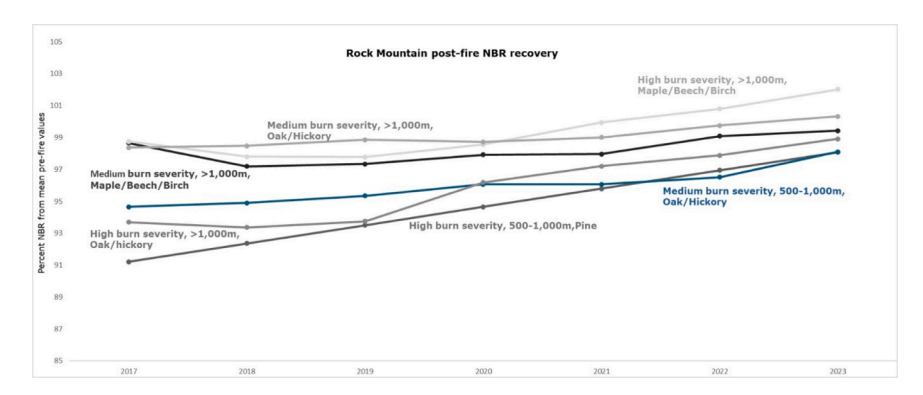


Fig. 9. Post-fire NBR recovery in sampled pixels stratified by burn severity, elevation classes, and vegetation/forest group, Rock Mountain Wildfire (Tallulah Watershed).

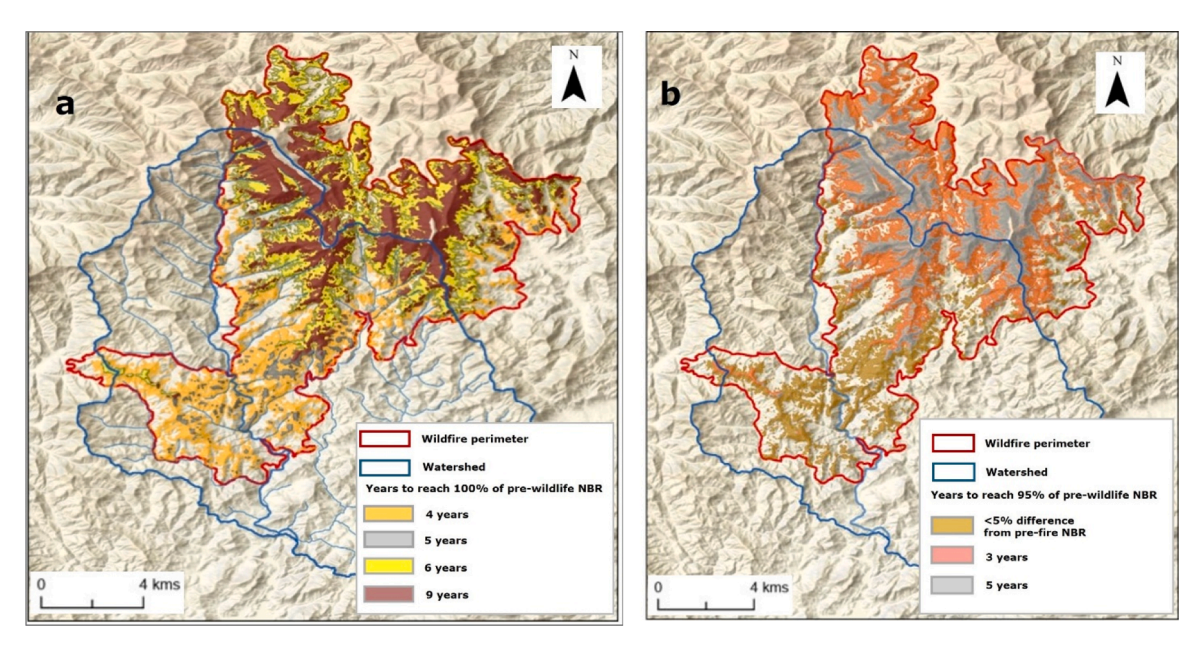


Fig. 10. Estimated time to NBR recovery post-wildfire, based on pre-fire mean NBR values – a)Years to reach 99 % of pre-fire NBR values; b) Years to reach 95 % of pre-fire NBR values.

et al., 2016). NBR and other vegetation indices based on short-wave infrared (SWIR) and new infrared (NIR) wavelengths have proven good performance in characterizing fire severity and post-fire recovery, especially when pre-fire images are used to quantify changes as RdNBR (Hislop et al., 2018; Kennedy et al., 2010). However, vegetation recovery based on observations of greenness through remote sensing may not indicate true forest recovery and the ecosystem processes associated with forest.

The growing volume of remotely sensed data also provides new opportunities for distinguishing forest recovery from other vegetation recovery. Combining data from multispectral instruments with datasets from different sensors, such as forest canopy height based on the Global Ecosystem Dynamics Investigation lidar instrument (Potapov et al., 2021) enables vegetation structure.

#### 4.2. Fire and vegetation recovery impacts on water yield

Post-fire water yield is generally expected to follow a hydrologic recovery pathway with a sequence of vegetation decline followed by increases in water yield, vegetation re-growth and subsequent return to pre-fire water yield. Water use by vegetation increases with vegetation regrowth, and in watersheds where annual water yield increased following fires, annual streamflow gradually decreases annually to reach pre-fire levels.

Forest wildfire could also indirectly impact ecosystem resilience and hydrology through lasting changes in vegetation composition and structure. Intense forest wildfires resulting in severe tree burning and high tree mortality could prompt a long-term shift in post-fire vegetation species composition from mesophytic (drought and fire intolerant) to xerophytic (drought and fire tolerant) species, resulting in lower evapotranspiration and potentially higher water yield (Caldwell et al., 2020, 2016). For example, Caldwell et al. (2020) found there was significantly greater mortality of mesophytic (mean 48.9  $\% \pm 4.2 \%$ ) than xerophytic (mean 28.6 %  $\pm$  3.8 %) trees of all sizes in the second year after the 2016 Camp Branch and Tellico Fires in the southern Appalachians. Caldwell et al. (2016) showed that shifts in species composition from mostly xerophytic to mesophytic species in the region over the 20th century resulted in increases in evapotranspiration and decreases in water yield. Thus the preferential mortality of mesophytic species in the 2016 wildfires could alter watershed water balances in a

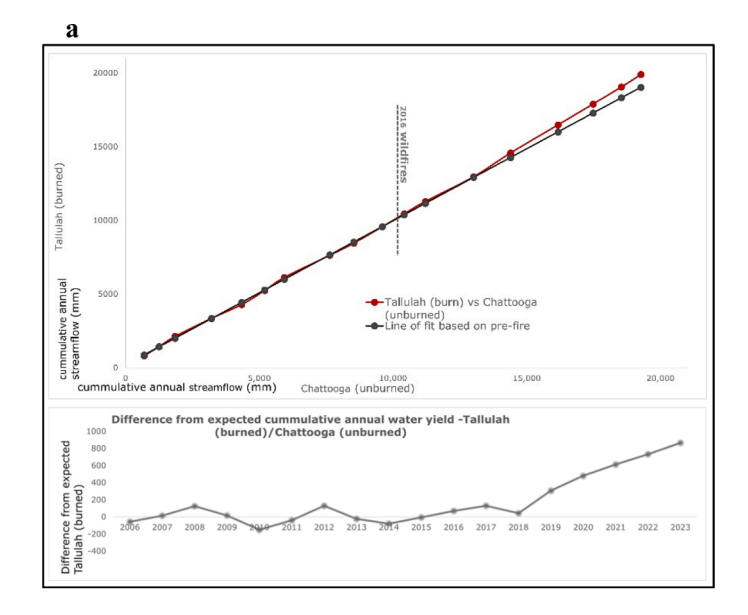
region that is critical to water supply (Caldwell et al., 2016). While there are differences in vegetation composition across and within the wildfire perimeters due to elevation, climate, and management, vegetation in SAE has generally shifted to species less adapted to fires (Caldwell, 2016; Elliott and Swank, 2008; Elliott and Vose, 2011).

Under increasing frequency and intensity of drought coupled with potential increases in wildfire frequency and severity, drought and wildfires could push forests in the region to a more xerophytic species composition, a condition that could increase forest resilience to these stressors in the long term (Vose and Elliott, 2016). However, the transition to these forest types without management (e.g., selective removal of mesophytic species, thinning, prescribed fire) could result in decades of degraded, less vigorous, and poorer quality forest stands (Vose and Elliott, 2016).

Historical analysis of streamflow reveals detectable differences between the similar Tallulah (burned), Chattooga and Hiwassee (paired, unburned) watersheds within a five-year window following the 2016 wildfire event. Residual cumulative streamflow indicates an increase in post-fire annual Tallulah streamflow. Since annual cumulative rainfall was similar in the paired watersheds, the change in residuals can be considered as the possible effect of the 2016 Rock Mountain fire in Tallulah watershed.

A detected change point in annual streamflow at Tallulah occurred in 2018, a year after a drop in NBR values within the Rock Mountain wildfire perimeter. In 2019 and 2020, increased annual streamflow exceeded expected values when compared with the paired watersheds Chattooga and Hiwassee at the highest levels for the period of record considered (1990–2023). NBR values returned to pre-fire values five to seven years following the wildfires, with timing for over 90 % NBR recovery corresponding to 2021–2022 and lower differences in streamflow between paired catchments.

Considering burn severity and vegetation recovery results, this study's findings of changes in annual water yield within the burned Tallulah watershed are intriguing. Annual water yield was found to have increased significantly at Tallulah using several methods (paired watershed analysis, change point analysis) when compared with multiple paired unburned watersheds, and remained consistently higher than expected six years following the 2016 wildfires. This appears to confirm that post-fire annual water yield generally increases following forest disturbance that impacts over 20 % of the watershed area, which



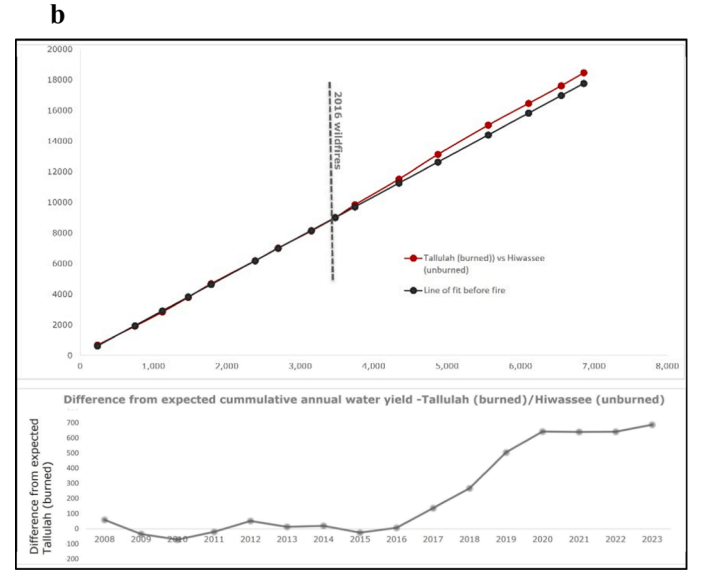


**Fig. 11.** Double mass analysis comparing cumulative annual water yield from the Tallulah (burned) watershed to the unburned Chattooga watershed (a) and the unburned Hiwassee watershed (b).

is consistent with numerous studies (Hallema et al., 2018). However, in the literature specifically focused on changes in water yield following wildfires in the western US, increased water yield was only found in case studies of watersheds with fire perimeters over half or more of the drainage area (Moreno and Hernan, 2020; Kinoshita and Hogue, 2015).

Water yield response to wildfire has been shown to be related to the proportion of the watershed area burned (Hallema et al., 2018) as well as the proportion of the watershed area burned at high severity (Caldwell et al., 2020). Hallema et al. (2018) identified a threshold of watershed burn area of 19 % as the lower bound at which a hydrologic response may be reasonably detected (Hallema et al., 2018). The Talullah watershed was burned over 35 % of it's area, with 13 % burned at high severity. Our results show that wildfire may have increased annual water yield in the Tallulah watershed by as much as 359 mm (29 %) and 295 mm (22 %) using the Chatooga and Hiawassee reference watersheds, respectively. These results are consistent with those of Caldwell et al. (2020), where a watershed in the SAE that had 65 % of it's area burned at high severity had 422 mm (39 %) great annual water yield post-fire than a paired unburned watershed. By comparison, with

the exception of coniferous-dominated Pacific Northwest watersheds, wildfires in the western US tend to result in larger relative changes but smaller absolute changes in water yield for a given proportion of watershed burned due to the generally drier climate and lower water yield (Hallema et al., 2018). For example, Blount et al. (2019) detected a 136 mm (140 %) increase in water yield in a catchment in Montana that was 90 % burned. This eastern vs. western US water yield response is true of forest disturbances generally (e.g., harvests).

In addition to the magnitude of the response in water yield, the time to water yield recovery varies regionally. We showed that water yield in the burned Talullah watershed returned to pre-burn levels after approximately five years after the fire and three years after the initial significant increase in water yield. This time to recovery is consistent with forest harvesting studies in the region. For example, Swank et al. (2014) showed that a water yield in a complete watershed clear-cut at the Coweeta Hydrologic Laboratory returned to pre-harvest levels after five years. The recovery in the Talullah watershed was found to be shorter than in most other studies focused on Western U.S wildfires (Guz et al., 2022, Meng et al., 2018, Zhao et al., 2016). A reasonable explanation for this difference in recovery time is related to the fact that biomass accumulation and post-disturbance forest recovery is influenced by climatic factors (Anderson et al., 2006) with slower recovery in arid forests and in colder, more humid forests as compared to Southern Appalachian forests. Given the variability in the magnitude and time to recovery of water yield response to wildfire, our results may not be applicable to burned watersheds in other hydroclimatic settings.

In addition to the magnitude of the response in water yield, the time to water yield recovery varies regionally. We showed that water yield in the burned Talullah watershed returned to pre-burn levels after approximately five years after the fire and three years after the initial significant increase in water yield. This time to recovery is consistent with forest harvesting studies in the region. For example, Swank et al. (2014) showed that a water yield in a complete watershed clear-cut at the Coweeta Hydrologic Laboratory returned to pre-harvest levels after five years. The recovery in the Talullah watershed was found to be shorter than in most other studies focused on Western U.S wildfires (Guz et al., 2022, Meng et al., 2018, Zhao et al., 2016). A reasonable explanation for this difference in recovery time is related to the fact that biomass accumulation and post-disturbance forest recovery is influenced by climatic factors (Anderson et al., 2006) with slower recovery in arid forests and in colder, more humid forests as compared to Southern Appalachian forests. Given the variability in the magnitude and time to recovery of water yield response to wildfire, our results may not be applicable to burned watersheds in other hydroclimatic settings.

While 35 % of the Tallulah watershed was impacted by wildfire, only 13 % of the Tallulah Rock Mountain fire perimeter was classified as high burn severity and yet up to a 25 % increase in water yield was detected. Caldwell et al. (2020) also detected increases in water yield from burned watersheds that had as low as 21 % of their drainage area burned at high severity. This suggests that studies focused on wildfires in the Western U. S. may not be easily extrapolated to the 2016 SAE fires, possibly due to climatic factors, differences in vegetation species and the infrequent occurrence of fires in the Eastern U.S. However, changes in water yield suggest a similar hydrologic recovery pathway with a sequence of vegetation decline followed by increases in water yield, vegetation re-growth and subsequent return to lower - although remaining consistently above pre-fire - water yield. This is most evident in the annual NBR trajectory as a percentage of pre-fire levels and the annual difference from expected streamflow at Tallulah (Fig. 12).

## 4.3. Implications for management

The fire regime in the SAE is projected to shift under increased drought conditions driven by climate change, resulting in more frequent fires and larger burned areas (Robbins et al., 2024). Given the potential for significant short and long-term water supply impacts following forest

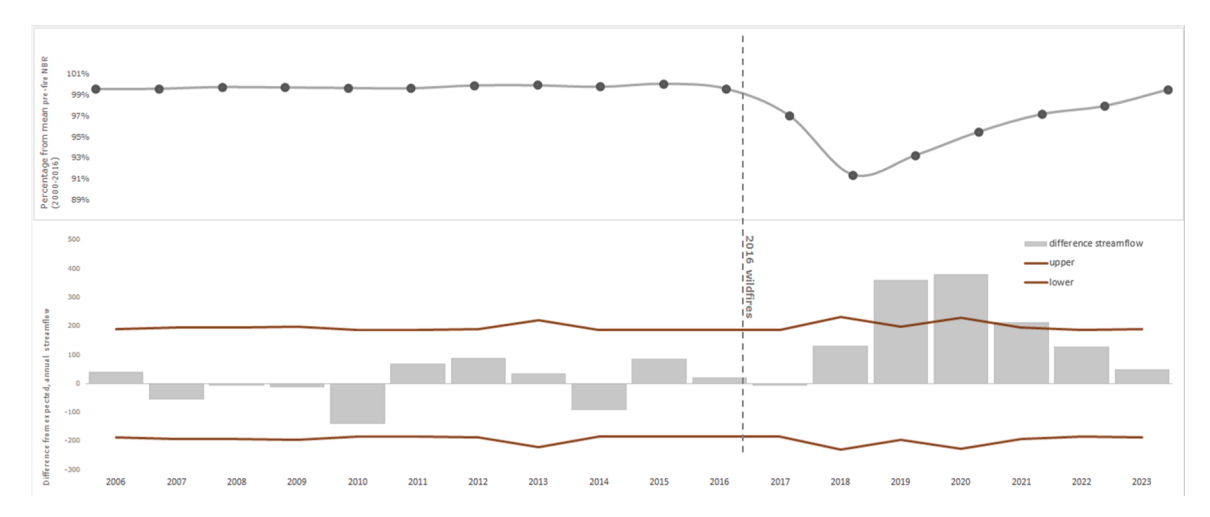


Fig. 12. a) Annual percentage from mean pre-fire NBR fitted values within Tallulah watershed burned areas and b) Difference from expected in annual streamflow at Tallulah (based on paired watershed Chattooga).

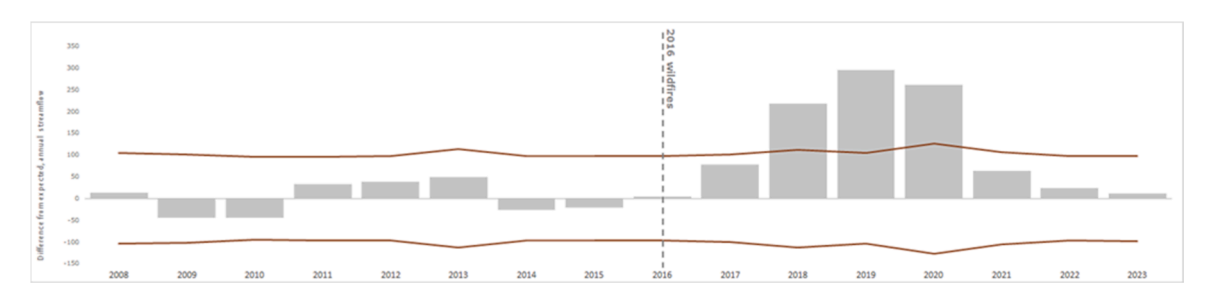


Fig. 13. Difference from expected in annual streamflow at Tallulah (based on paired watershed Hiwassee).

disturbance and especially fires, managers need access to reliable methods, data and tools to interpret and anticipate the potential effects of fire-driven forest disturbance on watershed vegetation and hydrology. These effects have been historically under-studied in regions with low fire frequency.

This study presents novel results that provide managers with the ability to estimate burn severity through remote sensing across a large ecoregion, to determine the timeframe for post-fire vegetation recovery, and to detect and quantify the effect of wildfire on annual water yield and hydrologic recovery.

Managers can use this information to anticipate potential wildfire impacts and to plan for adaptive forest management and preventive interventions, including prescribed fires and management of forest fuel loads. Managers can also use new scientific information regarding the effects of infrequent fires to plan for post-fire forest management interventions aimed at increasing forest resilience and maintaining a reliable water supply. This improved knowledge is increasingly important for managers planning for rapidly shifting fire regimes and anticipated increases in wildfire frequency associated with climate change.

#### 4.4. Limitations and opportunities for future research

This study had some limitations that could impact transferability of results to other watersheds and regions. First, there was limited availability of field observations of pre-fire and post-fire vegetation species to inform vegetation recovery trajectories derived from remotely sensed data in Tallulah watershed. Field observations could inform estimates of tree canopy recovery as compared to understory vegetation. Second, examination of fine-scale climate variables could provide additional context to the vegetation and hydrologic recovery results presented in this study. However, there are significant challenges in evaluating fine-spatial resolution climatic variables in this region, including 1) there is a

limited network of climate stations available, 2) the mountainous terrain causes high spatial variability in climate variables even over short distances limiting applicability of available climate stations, and 3) gridded climate data products that leverage observed climate variables to extrapolate across the region, such as Parameter-elevation Regressions on Independent Slopes Model (PRISM) and DAYMET gridded products often have difficulty in estimating climate variables due to their fine scale spatial variability (Behnke et al., 2016). Due to these limitations, we did not attempt to consider fine-scale climate data as potential explanatory variables in our assessment of vegetation and hydrologic recovery. Third, there were limitations related to modeling burn severity using remotely sensed data over large areas with frequent cloud coverage. This study employed cloud masking and image reducers to alleviate limitations related to frequent cloud cover in the SAE Ecoregion.

And lastly, there was limited availability of pre-fire and post-fire hydrologic records for other SAE watersheds impacted by the 2016 wildfire. A limited number of reference watersheds are suitable for analyzing wildfire impacts, due to human disturbance and gaps in continuous daily streamflow data collection. Additionally, watersheds rarely overlap with wildfire burned areas, due to the smaller size of wildfire in the Eastern U.S. The study approach combined established methods to yield realistic and explainable results while alleviating these limitations.

The focus of this study was to improve understanding of infrequent wildfire impacts on vegetation and catchment dynamics in an understudied region, with the goal to augment the data and tools available for managers, which enhances their ability to respond and plan to future fire events. Areas of future research could include combining vegetation indices at different spatial resolutions with field observations to address knowledge gaps in post-fire vegetation re-growth. Future studies in impacted watersheds with limited records or ungauged could inform

planning to concomitantly reduce the risk of fires while improving the effectiveness of post-fire forest management actions to maintain water supplies. Lastly, future modeling efforts could explore the contribution of climate variables to variations in vegetation response at fine spatial and temporal resolution.

#### 5. Conclusions

This study revealed opportunities for efficient cloud-computing estimates of high and moderate burn severity and vegetation recovery trends across multiple wildfire perimeters following the 2016 fire outbreak in the Southern Appalachian Ecoregion, and linked those trends to post-wildfire water yield in a burned forested watershed. This work is among the very few to make these connections between wildfire, vegetation disturbance, and recovery, and ecosystem processes in the eastern U.S.

Changes in annual streamflow in a burned watershed were detected following wildfire through paired comparison with multiple unburned watersheds, suggesting an increase and recovery in annual water yield that coincided with vegetation disturbance and subsequent recovery as detected through remote sensing. Despite limitations related to a small sample size of hydrologic response and linkages between remotely-sensed greenness and forest ecosystem recovery, this study advances our understanding of how infrequent fires can impact catchment vegetation and hydrology in an understudied region. Future work can leverage these findings by examining additional watershed and collecting field data to evaluate vegetation recovery across broad regions of the eastern U.S. The improved understanding provided by this study augments the ability of managers to plan for an expected increase in the frequency of forest fires and to anticipate the impacts on forested mountain catchments and on water provision from these catchments.

#### CRediT authorship contribution statement

**I. Bouvier:** Writing – original draft, Methodology, Formal analysis, Data curation, Conceptualization. **P. Caldwell:** Writing – review & editing, Methodology. P. Houser: Writing – review & editing.

#### **Funding statement**

This research did not receive any specific grant from funding agencies in the public, commercial, or not-for-profit sectors.

## **Declaration of Competing Interest**

The authors declare that they have no known competing financial interests or personal relationships that could have appeared to influence the work reported in this paper. Any opinions, findings, conclusions, or recommendations expressed in the material are those of the authors and do not necessarily reflect the views of the USDA or George Mason University. Any use of trade, firm, or product names is for descriptive purposes only and does not imply endorsement by the U.S. Government.

#### Acknowledgments

We thank Dr. Ning Liu for guidance in developing NBR burn severity models. We thank Dr. Katherine Elliott and Joel Scott for oversight, collection, and analysis of plot-level measurements used to estimate burn severity.

## **Data Availability**

Datasets that support the findings of this study are openly available in Zenodo at:  $https://doi.org/10.5281/zenodo.14884171 \ Plot field \ data$  are available on request.

#### References

- Anderson, Kristina J., et al., 2006. Temperature-dependence of biomass accumulation rates during secondary succession. Ecol. Lett. 9 (6), 673–682.
- Anderson, Mark, et al., 2013. Southern blue ridge: an analysis of matrix forests. Nat. Conserv.
- Arthur, Mary A., et al., 2021. Fire ecology and management in eastern broadleaf and Appalachian forests. Fire Ecol. Manag. Present Future US For. Ecosyst. 105–147.
- Bartels, Samuel F., et al., 2016. Trends in post-disturbance recovery rates of Canada's forests following wildfire and harvest. For. Ecol. Manag. 361, 194–207.
- Behnke, R., et al., 2016. Evaluation of downscaled, gridded climate data for the conterminous United States. Ecol. Appl. 26 (5), 1338–1351.
- Biederman, Joel A., et al., 2015. Recent tree die-off has little effect on streamflow in contrast to expected increases from historical studies. Water Resour. Res. 51 (12), 9775–9789.
- Blount, K., Ruybal, C.J., Franz, K.J., Hogue, T.S., 2019. Increased water yield and altered water partitioning follow wildfire in a forested catchment in the western United States. Ecohydrology 13, e2170. https://doi.org/10.1002/eco.2170.
- Bright, Benjamin C., et al., 2019. Examining post-fire vegetation recovery with Landsat time series analysis in three western North American forest types. Fire Ecol. 15 (1), 1–14
- Burt, T.P., McDonnell, J.J., 2015. Whither field hydrology? The need for discovery science and outrageous hydrological hypotheses. Water Resour. Res. 51, 5919–5928. https://doi.org/10.1002/2014WR016839.
- Caldwell, Peter V., et al., 2016. Declining water yield from forested mountain watersheds in response to climate change and forest mesophication. Glob. Change Biol. 22 (9), 2997–3012.
- Caldwell, Peter V., et al., 2020. Watershed-scale vegetation, water quantity, and water quality responses to wildfire in the southern Appalachian Mountain region, United States. Hydrol. Process. 34 (26), 5188–5209.
- Cardil, Adrián, et al., 2019. Fire and burn severity assessment: calibration of relative differenced normalized burn ratio (RdNBR) with field data. J. Environ. Manag. 235, 342–349
- Carta, Francesco, et al., 2023. "Advancements in forest fire prevention: A comprehensive survey. Sensors 23 (14), 6635.
- Chen, Yang, Morton, Douglas C., Randerson, James T., 2024. Remote sensing for wildfire monitoring: insights into burned area, emissions, and fire dynamics. One Earth 7 (6), 1022–1028
- De Cicco, L.A., Hirsch, R.M., Lorenz, D., Watkins, W.D., Johnson, M., 2024, dataRetrieval: R packages for discovering and retrieving water data available from Federal hydrologic web services, v.2.7.15, doi:10.5066/P9X4L3GE.
- Eidenshink, Jeff, et al., 2007. "A project for monitoring trends in burn severity. Fire Ecol. 3, 3–21
- Elliott, Katherine J., Swank, Wayne T., 2008. Long-term changes in forest composition and diversity following early logging (1919–1923) and the decline of American chestnut (Castanea dentata). Plant Ecol. 197 (2), 155–172.
- Elliott, Katherine J., Vose, James M., 2011. The contribution of the Coweeta Hydrologic Laboratory to developing an understanding of long-term (1934–2008) changes in managed and unmanaged forests. For. Ecol. Manag. 261 (5), 900–910.
- Falcone, James A. GAGES-II: Geospatial attributes of gages for evaluating streamflow. US Geological Survey, 2011.
- European Space Agency, 2024. Sentinel-2 MultiSpectral Instrument. Copernicus.
- Ford, Chelcy R., et al., 2011. Can forest management be used to sustain water-based ecosystem services in the face of climate change? Ecol. Appl. 21 (6), 2049–2067.
- Forzieri, Giovanni, et al., 2022. Emerging signals of declining forest resilience under climate change. Nature 608 (7923), 534–539.
- Goetz J., Schwarz C. (2023). fasstr: Analyze, Summarize, and Visualize Daily Streamflow Data. https://bcgov.github.io/fasstr/, https://github.com/bcgov/fasstr.
- Gorelick, N., Hancher, M., Dixon, M., Ilyushchenko, S., Thau, D., Moore, R., 2017. Google Earth Engine: planetary-scale geospatial analysis for every-one. Remote Sens. Environ. 202, 18–27.
- Guz, Jaclyn, Sangermano, Florencia, Kulakowski, Dominik, 2022. The influence of burn severity on post-fire spectral recovery of three fires in the Southern Rocky Mountains. Remote Sens. 14 (6), 1363.
- Hallema, Dennis W., et al., 2018. Burned forests impact water supplies. Nat. Commun. 9 (1), 1307.
- Hislop, Samuel, et al., 2018. Using landsat spectral indices in time-series to assess wildfire disturbance and recovery. Remote Sens. 10 (3), 460.
- Kendall, Maurice George. "Rank correlation methods." (1948).
- Kennedy, Robert E., et al., 2018. Implementation of the LandTrendr algorithm on google earth engine. Remote Sens. 10 (5), 691.
- Kennedy, Robert E., Yang, Zhiqiang, Cohen, Warren B., 2010. Detecting trends in forest disturbance and recovery using yearly Landsat time series: 1. LandTrendr—Temporal segmentation algorithms. Remote Sens. Environ. 114 (12),
- LandTrendr—Temporal segmentation algorithms. Remote Sens. Environ. 114 (12) 2897–2910.Key, Carl H., Nathan, C.Benson, 2006. Landscape assessment (LA). FIREMON Fire Eff.
- Monit. Inventory Syst. 164. LA-1.

  Kinoshita, Alicia M., Hogue, Terri S., 2015. Increased dry season water yield in burned watersheds in Southern California. Environ. Res. Lett. 10 (1), 014003.
- Lafon, Charles W., et al. Fire history of the Appalachian region: a review and synthesis. (2017).
- Lins, Harry F. USGS hydro-climatic data network 2009 (HCDN-2009). No. 2012-3047. US Geological Survey, 2012.

- Masek, J., Ju, J., Roger, J., Skakun, S., Vermote, E., Claverie, M., Dungan, J., Yin, Z., Freitag, B., Justice, C. (2021). HLS Sentinel-2 Multi-spectral Instrument Surface Reflectance Daily Global 30m v2.0 [Data set]. NASA EOSDIS Land Processes Distributed Active Archive Center.
- Meng, Ran, et al., 2015. "Effects of fire severity and post-fire climate on short-term vegetation recovery of mixed-conifer and red fir forests in the Sierra Nevada Mountains of California. Remote Sens. Environ. 171, 311–325.
- Meng, Ran, Zhao, Feng, 2017. Remote sensing of fire effects: a review for recent advances in burned area and burn severity mapping. Remote Sens. Hydrometeorol. Hazards 261–283.
- Meng, Ran, et al., 2018. "Measuring short-term post-fire forest recovery across a burn severity gradient in a mixed pine-oak forest using multi-sensor remote sensing techniques. Remote Sens. Environ. 210, 282–296.
- Miller, Jay D., Thode, Andrea E., 2007. Quantifying burn severity in a heterogeneous landscape with a relative version of the delta Normalized Burn Ratio (dNBR). Remote Sens. Environ. 109 (1), 66–80.
- Moreno, Hernan A., et al., 2020. Utility of satellite-derived burn severity to study shortand long-term effects of wildfire on streamflow at the basin scale. J. Hydrol. 580,
- Partington, Daniel, et al., 2022. Predicting wildfire induced changes to runoff: A review and synthesis of modeling approaches. Wiley Interdiscip. Rev.: Water 9 (5), e1599.
- Pérez-Cabello, Fernando, Raquel Montorio, Alves, Daniel Borini, 2021. Remote sensing techniques to assess post-fire vegetation recovery. Curr. Opin. Environ. Sci. Health 21, 100251.
- Pickell, Paul D., et al., 2016. Forest recovery trends derived from Landsat time series for North American boreal forests. Int. J. Remote Sens. 37 (1), 138–149.
- Potapov, Peter, et al., 2021. Mapping global forest canopy height through integration of GEDI and Landsat data. Remote Sens. Environ. 253, 112165.
- Reilly, Matthew J., et al., 2022. Drivers and ecological impacts of a wildfire outbreak in the southern Appalachian Mountains after decades of fire exclusion. For. Ecol. Manag. 524, 120500.
- Robbins, Zachary J., et al., 2024. Fire regimes of the Southern Appalachians may radically shift under climate change. Fire Ecol. 20 (1), 1–17.
- Searcy, James Kincheon, Clayton, H.Hardison, 1960. Double-mass curves. US Government Printing Office.
- Seidl, Rupert, et al., 2017. Forest disturbances under climate change. Nat. Clim. Change 7 (6), 395–402.
- Simon, Steven A. Ecological zones in the Southern Appalachians: First approximation. Vol. 41. US Department of Agriculture, Forest Service, Southern Research Station, 2005.

- Srivastava, A., et al., 2020. Modeling forest management effects on water and sediment yield from nested, paired watersheds in the interior Pacific Northwest, USA using WEPP. Sci. Total Environ. 701, 134877.
- Swank, Wayne T., et al., 2014. Response and recovery of water yield and timing, stream sediment, abiotic parameters, and stream chemistry following logging. Long-Term Response of a Forest Watershed Ecosystem: Clearcutting in the Southern Appalachians (The Long-term Ecological Research Network Series), edited by: Swank, WT and Webster. JR, Oxford University Press, Oxford, UK, pp. 36–56.
- $\label{lem:u.s.} U.S.\ Geological Survey, (n.d)\ 3D\ Elevation\ Program\ 1-Meter\ Resolution\ Digital\ Elevation\ Model,\ 2020,\ URL\ \langle https://www.usgs.gov/the-national-map-data-delivery\rangle.$
- Valjarević, Aleksandar, 2024. GIS-based methods for identifying river networks types and changing river basins. Water Resour. Manag. 38 (13), 5323–5341.
- Van Lear, David H., 1989. 2013 History, uses, and effects of fire in the Appalachians, 54.

  US Department of Agriculture, Forest Service, Southeastern Forest Experiment
  Station
- Vose, James M., Elliott, Katherine J., 2016. Oak, fire, and global change in the eastern USA: what might the future hold?, 20 p Fire Ecol. 12 (2), 160–179. https://doi.org/ 10.4996/fireecology.1202160.
- Vujović, Filip, et al., 2024. Geospatial modeling of wildfire susceptibility on a national scale in Montenegro: a comparative evaluation of F-AHP and FR methodologies. Open Geosci. 16 (1), 20220694.
- Whittaker, Robert H., 1956. Vegetation of the great smoky mountains. Ecol. Monogr. 26 (1), 2–80.
- Wimberly, Michael C., Reilly, Matthew J., 2007. Assessment of fire severity and species diversity in the southern Appalachians using Landsat TM and ETM+ imagery. Remote Sens. Environ. 108 (2), 189–197.
- Yang, Jia, et al., 2017. Continental scale quantification of post-fire vegetation greenness recovery in temperate and boreal North America. Remote Sens. Environ. 199, 277–290
- Yang, Songxi, Huang, Qunying, Yu, Manzhu, 2024. Advancements in remote sensing for active fire detection: a review of datasets and methods. Sci. Total Environ., 173273
- Zhang, Zhaoming, et al., 2021. Assessment of annual composite images obtained by Google Earth engine for urban areas mapping using random forest. Remote Sens. 13 (4), 748.
- Zhao, Feng R., et al., 2016. Long-term post-disturbance forest recovery in the greater Yellowstone ecosystem analyzed using Landsat time series stack. Remote Sens. 8 (11), 898.
- Zhao, Kaiguang, et al., 2019. Detecting change-point, trend, and seasonality in satellite time series data to track abrupt changes and nonlinear dynamics: a Bayesian ensemble algorithm. Remote Sens. Environ. 232, 111181.